BIOLOGICAL SCIENCES

OPEN ACCESS

ASTAXANTHIN AND CELLULAR METABOLITES PRODUCTION IN *HAEMATOCOCCUS LACUSTRIS* EXPOSED TO SILVER NANOPARTICLES

Liliana CEPOI[1], Ludmila RUDI[1], Tatiana CHIRIAC[1], Vera MISCU[1], Ecaterina PLINGAU[1]

[1] Technical University of Moldova, Institute of Microbiology and Biotechnology, Republic of Moldova

Coresponding author: Liliana Cepoi, e-mail: liliana.cepoi@imb.utm.md

https://doi.org/10.38045/ohrm.2026.1.06 CZU: 582.263:620.3:546.57

ABSTRACT

Introduction Silver nanoparticles (AgNPs) can modulate microalgal metabolism in a dose-dependent and stage-specific manner. *Haematococcus lacustris*, a key astaxanthin-producing microalga, is highly sensitive to environmental stressors that regulate the transition from the green vegetative stage to the red aplanospore stage.

Material and methods The effects of 10 nm and 20 nm citrate-stabilized AgNPs (0.01–5 mg L^{-1}) were assessed on biomass, cellular metabolites, photosynthetic pigments, lipids, and astaxanthin. Nanoparticles were introduced on day 3, with analyses performed at the end of the green (day 9) and red stages (day 16).

Results Low to moderate AgNPs concentrations (0.01–1 mg L^{-1}) increased biomass, proteins, carbohydrates, and lipids during the green stage, while 5 mg L^{-1} inhibited growth and pigments and elevated MDA levels. In the red stage, all concentrations reduced final biomass; however, 10 nm AgNPs at 0.01–0.5 mg L^{-1} boosted astaxanthin (by up to ~30%) and lipids (by up to ~96%). Higher doses, along with all 20 nm AgNP treatments, suppressed astaxanthin accumulation.

Conclusions *H. lacustris* exhibits a hormetic response to AgNPs: mild exposure stimulates key metabolites, while higher concentrations become inhibitory. Nanoparticle size, dose, and timing are crucial for precisely directing metabolic pathways and improving astaxanthin yield.

Keywords *Haematococcus lacustris*, silver nanoparticles, astaxanthin, metabolites, oxidative stress, hormesis.

ASTAXANTINA ȘI PRODUCEREA METABOLIȚILOR CELULARI ÎN *HAEMATOCOCCUS LACUSTRIS* EXPUS LA NANOPARTICULE DE ARGINT

Introducere Nanoparticulele de argint (AgNPs) pot modula metabolismul microalgelor într-un mod dependent de concentrație și de stadiul fiziologic. *Haematococcus lacustris*, un important producător de astaxantină, prezintă o sensibilitate sporită la factorii de stres care reglează tranziția de la faza de celule verzi vegetative la cea de aplanospori roșii.

Material și metode Au fost evaluate efectele AgNP-urilor de 10 nm și 20 nm (0,01–5 mg L^{-1}) asupra biomasei, metaboliților celulari, pigmenților fotosintetici, lipidelor și astaxantinei. Nanoparticulele au fost adăugate în ziua a 3-a, iar analizele au fost efectuate la sfârșitul fazei de celule vegetative (ziua a 9-a) și al fazei de aplanospori (ziua a 16-a).

Rezultate Concentrațiile mici și moderate de AgNPs (0,01–1 mg L^{-1}) au stimulat biomasa, proteinele, carbohidrații și lipidele în faza de celule vegetative, în timp ce 5 mg L^{-1}au inhibat creșterea și conținutul de pigmenți și au crescut nivelul MDA. În faza de aplanospori, toate concentrațiile au redus biomasa finală; totuși, AgNP de 10 nm la 0,01–0,5 mg L^{-1} au intensificat sinteza de astaxantină (până la ~30%) și de lipide (până la ~96%). Dozele mai mari și toate tratamentele cu AgNPs de 20 nm au redus semnificativ astaxantina.

Concluzii *H. lacustris* manifestă un răspuns hormetic la AgNPs: expunerea moderată stimulează metaboliții valoroși, în timp ce concentrațiile ridicate devin inhibitoare. Dimensiunea nanoparticulelor, doza aplicată și durata expuneriit constituie factori determinanți în modularea controlată a metabolismului celular și în optimizarea producției de astaxantină.

Cuvinte-cheie *Haematococcus lacustris*, nanoparticule de argint, astaxantină, metaboliți, stres oxidativ, răspuns hormetic.

INTRODUCTION

Nanotechnology is among the most dynamic frontiers of modern science, with applications expanding from engineering to biomedicine. This growth is driven by the unique physicochemical properties of nanomaterials, including nanoscale dimensions, a high specific surface area, and enhanced reactivity (1, 2). As their use has broadened, so have concerns regarding their toxicological impact, as numerous studies indicate that some nanomaterials can induce oxidative stress, cellular damage, and systemic toxicity, particularly at high concentrations or in unsuitable formulations (3). At the same time, a deeper understanding of their mechanisms of action has shifted the focus from simply avoiding toxicity toward exploring their potential for the controlled, beneficial stimulation of cellular processes (4, 5). This new perspective has opened new nanobiotechnological applications, including those involving microalgae, where nanoparticles may modulate oxidative stress and enhance the biosynthesis of high-value metabolites such as lipids, carotenoids, proteins, and exopolysaccharides (6–8).

Despite increasing interest, the biological responses of microalgae to nanoparticle exposure remain poorly understood. These responses are highly variable, depending critically on nanoparticle type, concentration, and the physiological state of the organism. (6, 8, 9). Among different nanomaterials, silver nanoparticles (AgNPs) are particularly noteworthy because of their dual biological effects, where they can either stimulate or inhibit cellular processes, depending on size, concentration, and surface properties. When carefully controlled, moderate oxidative stress induced by AgNPs may act as a metabolic signa, promoting the synthesis of bioactive compounds (8, 10, 11).

The green microalga *Haematococcus lacustris* (formerly *Haematococcus pluvialis*) is a model organism in phycobiotechnology due to its exceptional capacity to accumulate astaxanthin, a carotenoid with strong antioxidant properties and significant pharmaceutical, nutraceutical, cosmetic, and aquaculture relevance (12–16). In addition to astaxanthin, *H. lacustris* produces considerable amounts of lipids, proteins, and carbohydrates, further enhancing its biotechnological value (12, 13).

The life cycle of *Haematococcus lacustris* consists of two distinct morphological and physiological stages: a vegetative green stage and a red aplanospore (or cyst) stage, with the latter characterized by the extensive accumulation of carotenoids. These stages also differ structurally. Green vegetative cells possess a relatively fragile cell wall that allows the direct extraction of intracellular components. In contrast, red aplanospores develop a thick, resilient cell wall that, while providing protection, substantially complicates metabolite extraction, requiring specific cell disruption or pretreatment procedures. Due to these structural and functional differences, each stage must be evaluated separately, when assessing nanoparticle effects on growth and metabolite biosynthesis – particularly in the case of astaxanthin (13, 17–21).

In this context, this study examines the impact of silver nanoparticles on astaxanthin accumulation and cellular metabolite profiles in *Haematococcus lacustris* CNMN-AV-05, specifically comparing its green

and red developmental stages. The responses to 10 and 20 nm AgNPs were evaluated by measuring biomass, major biochemical components, lipids, and astaxanthin, in order to clarify how nanoparticle exposure influences growth and metabolism across the two developmental stages.

MATERIALS AND METHODS

Microalgal Strain and Culture Conditions

The green microalga *Haematococcus lacustris* CNMN-AV-05 (NCNM, Technical University of Moldova) was used in all experiments. Starter cultures were maintained as aplanospores under continuous illumination (150 $\mu mol \cdot m^{-2} \cdot s^{-1}$, measured using a quantum light meter, LI-250A, LI-COR Biosciences, USA) at 26–28 °C in the mineral medium described below.

For experimental assays, cultures were inoculated at 0.2 g $DW \cdot L^{-1}$ in 50 mL working volumes (100 mL Erlenmeyer flasks) and cultivated under continuous light (75 $\mu mol \cdot m^{-2} \cdot s^{-1}$) with shaking twice daily during 10 min. The medium pH remained stable (6.8–7.0). The mineral medium contained ($g \cdot L^{-1}$): $NaNO_3$ 0.3; KH_2PO_4 0.02; K_2HPO_4 0.08; $MgSO_4 \cdot 7H_2O$ 0.01; $ZnSO_4 \cdot 7H_2O$ 0.0001; $MnSO_4 \cdot 5H_2O$ 0.0015; $CuSO_4 \cdot 5H_2O$ 0.00008; H_3BO_3 0.0003; $(NH_4)_6Mo_7O_{24} \cdot 4H_2O$ 0.0003; $Fe_2(SO_4)_3$ 0.013; EDTA 0.0075.

Silver Nanoparticles

Citrate-stabilized silver nanoparticles (AgNPs) of 10 nm (Lot MKCK8345) and 20 nm (Lot MKCM2276) were obtained from Sigma-Aldrich (Optical Density (OD) = 1; Polydispersity Index (PDI) < 0.2; TEM-verified size ±0.2 nm). Prior to use, stock suspensions were vortexed and briefly sonicated, then diluted in sterile medium immediately before addition to cultures.

After introduction, AgNPs remained visually stable throughout the experiment, with no sedimentation, flocculation; given the low working concentrations, no optical effects were expected. Seven concentrations were tested: 0, 0.01, 0.05, 0.1, 0.5, 1.0, and 5 $mg \cdot L^{-1}$. Nanoparticles were added on day 3, at the transition from germination to the green vegetative stage.

Experimental Design

Two experimental series were conducted – one for each AgNP size (10 nm and 20 nm).

For each concentration, three independent replicates were prepared for each sampling time.

Biomass was harvested at day 9 – end of the green vegetative stage, and at day 16 – end of the red aplanospore stage (after increasing illumination to 150 $\mu mol \cdot m^{-2} \cdot s^{-1}$ from day 14 to induce carotenoid accumulation).

After harvesting, biomass was washed with distilled water and resuspended to a standard concentration of 10 $mg \cdot mL^{-1}$ for biochemical assays.

Sample Preparation for Biochemical Analyses

Due to structural differences between stages, biomass was processed as follows:

a) Green stage (motile cells) – biomass subjected to three freeze–thaw cycles (–20 °C / +25 °C) to disrupt cells; homogenates used for protein, carbohydrate, pigment, lipid, and MDA assays.

b) Red stage (aplanospores) – aplanospores possess a thick, resistant wall; therefore biomass was subjected to acid hydrolysis (0.1 M HCl, 90 °C, 10 min), washed 3× with water, the pellet was used for astaxanthin extraction, residual material was used for lipid quantification.

Biomass Quantification

Biomass concentration was determined spectrophotometrically at 680 nm (green cells) and 565 nm (red aplanospores). Calibration curves were constructed separately for each cell type within the OD range 0.01–0.40 (7-point curves; $R^2 > 0.99$), and samples were diluted with fresh medium to fall within this linear interval.

Biochemical Analyses

Biochemical assays were performed on biomass standardized to 10 mg/mL, with cell disruption adapted to each stage: freeze–thaw cycles for green cells and mild acid hydrolysis (0.1 M HCl, 90°C, 10 min) for aplanospores.

Protein content was measured using a modified Folin–Ciocalteu assay (22). Absorbance was recorded at 750 nm, and concentrations were calculated from a BSA calibration curve.

Total carbohydrates were quantified by the anthrone method, heating samples with anthrone–H_2SO_4 and reading absorbance at 620 nm, using a glucose calibration curve.

Pigments (chlorophylls and carotenoids) were extracted in 96% ethanol, and absorbance at 649, 665, and 450 nm was used to calculate chlorophyll *a*, chlorophyll *b*, and total carotenoids according to Lichtenthaler (1987) (23).

Total lipids were quantified by the phosphovanillin colorimetric method (24). Green-stage biomass was extracted with chloroform–ethanol; for red-stage biomass, lipids were measured from the residue remaining after astaxanthin extraction. Absorbance was measured at 520 nm, and lipid content was determined using an oleic acid standard curve.

Lipid peroxidation was assessed via the Thiobarbituric Acid-Malondialdehyde (TBA–MDA) assay, measuring absorbance at 535 nm (corrected at 600 nm). MDA content was calculated using $\varepsilon = 1.56 \times 10^5\ M^{-1} \cdot cm^{-1}$.

Astaxanthin was extracted from hydrolyzed aplanospores with 96% ethanol, and absorbance at 478 nm was converted to concentration using a calibration curve of pure astaxanthin (≥97%).

Statistical Analysis

All experiments were performed in triplicate, and results are expressed as mean ± standard deviation (SD). Statistical differences between treatments and controls were assessed using one-way ANOVA, followed by Welch's t-test for unequal variances. Differences were considered statistically significant at $p < 0.05$.

RESULTS

Effects of AgNPs on Biomass and Cellular Metabolites of *Haematococcus lacustris* in the Green Stage

Exposure of *H. lacustris* to silver nanoparticles produced clear, concentration-dependent changes in biomass and cellular metabolite content at the end of the green growth phase (fig. 1–4). In terms of growth (fig. 1), both 10 nm and 20 nm AgNPs stimulated biomass accumulation at low and moderate concentrations.

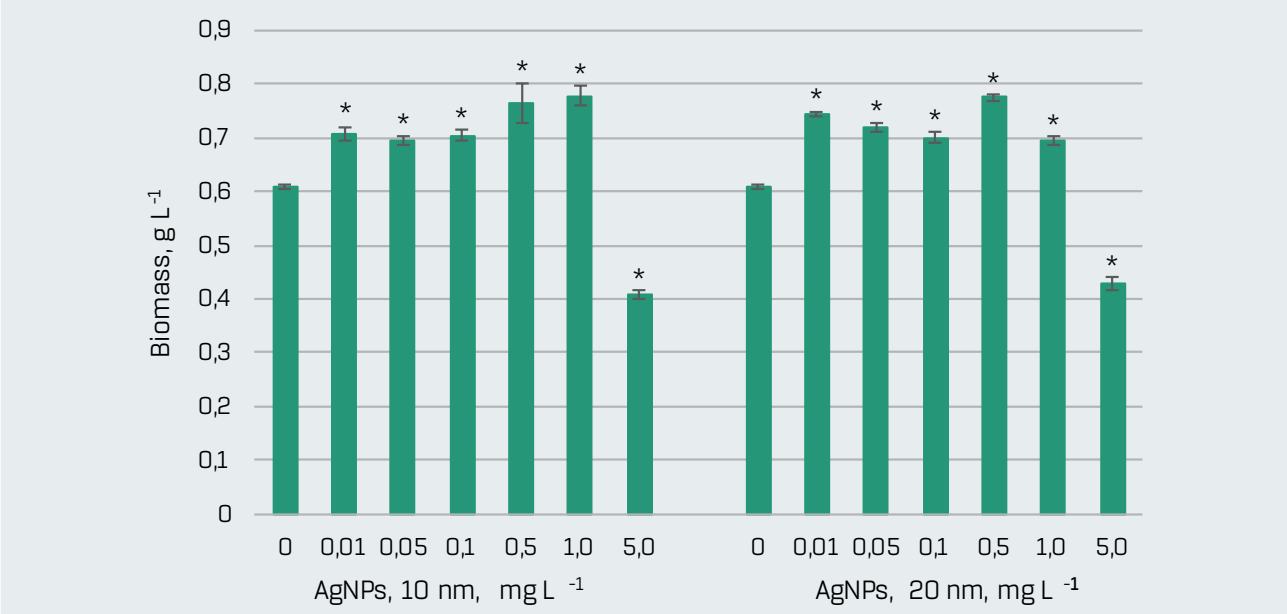

Figure 1. Biomass (g L^{-1}) of *Haematococcus lacustris* accumulated during the green stage following exposure to 10 nm and 20 nm AgNPs at various concentrations (mg L^{-1}). 0 – control; data are presented as mean ± SD (n = 3). Statistical significance is indicated relative to the control: * – $p < 0.05$.

For 10 nm AgNPs, 0.01–0.1 mg L^{-1} increased biomass by ~14–16%, while 0.5–1.0 mg L^{-1}produced stronger stimulation, up to ~26–28% above the control. A similar pattern was observed for 20 nm AgNPs, with biomass increases of ~14% at 0.01 mg L-1 and ~27% at 0.5–1.0 mg L^{-1}. In contrast, the highest concentration (5.0 mg L^{-1}) inhibited growth,

reducing biomass by ~30–33% for both nanoparticle sizes. Thus, AgNPs enhanced green-stage biomass within an optimal concentration window, while excessive doses were clearly detrimental.

Protein and carbohydrate contents also responded positively to AgNP treatment, although with different sensitivities (fig. 2). For proteins, all tested concentrations of both 10 nm and 20 nm AgNPs led to significant increases relative to the control. In cultures treated with 10 nm AgNPs, protein content rose by ~9–16%, with the strongest effects at 0.1–1.0 mg L^{-1}. For 20 nm AgNPs, the stimulatory effect was more pronounced, with increases of ~14–25% in the same concentration range, indicating that both size and dose influence protein accumulation.

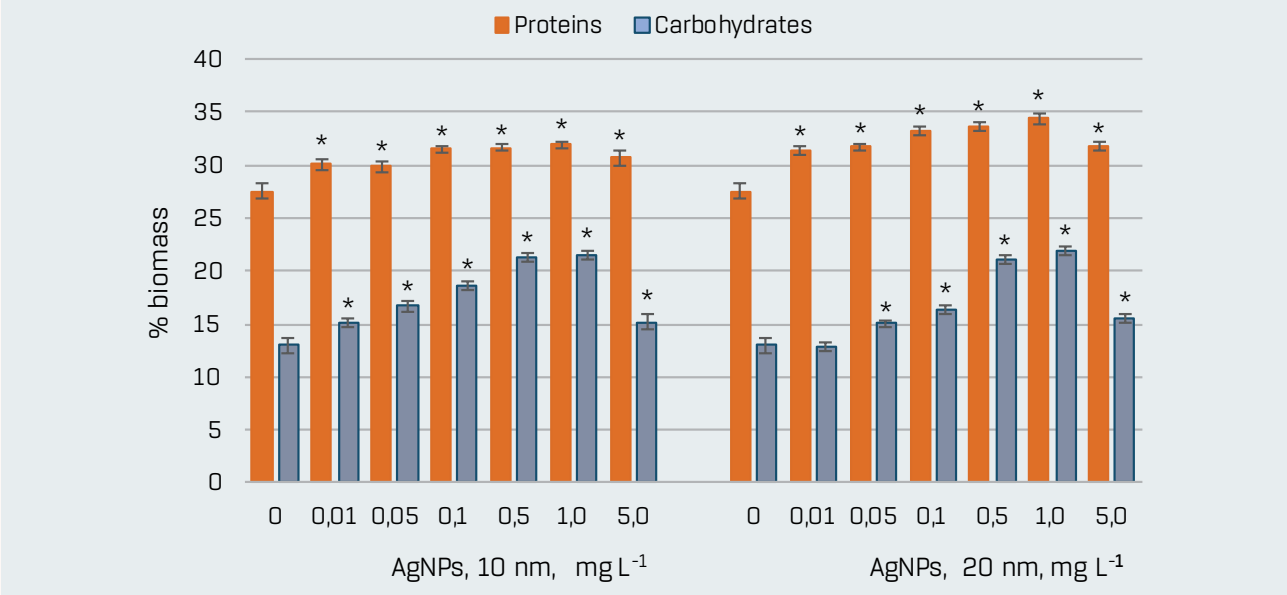

Figure 2. Protein and carbohydrate content (% of biomass) in *Haematococcus lacustris* collected at the end of the green phase after exposure to 10 nm and 20 nm AgNPs (mg L^{-1}). 0 = control; mean ± SD (n = 3); * $p < 0.05$ vs. control.

Carbohydrates displayed an even more marked stimulation. In the presence of 10 nm AgNPs, carbohydrate content increased at all concentrations, with moderate rises (~16%) at 0.01 and 5.0 mg L-1 and stronger enhancement (up to ~65%) at 0.05–1.0 mg/L. Treatment with 20 nm AgNPs similarly elevated carbohydrate levels at 0.05–5.0 mg L^{-1}, with maximal increases of ~62–68% at 0.5–1.0 mg L^{-1}, while 0.01 mg L^{-1} induced no detectable change. Overall, these results indicate that AgNPs, particularly in the intermediate range of 0.05–1.0 mg L^{-1}, strongly stimulate primary carbon storage in the green stage.

The pigment profile was more sensitive to AgNP exposure, especially at higher concentrations (fig. 3). For 10 nm AgNPs, total chlorophyll content remained comparable to the control at 0.01–0.5 mg L^{-1}, but declined by ~16% at 1.0 mg L^{-1} and ~29% at 5.0 mg L^{-1}. In cultures treated with 20 nm AgNPs, 0.01–0.05 mg L^{-1} had little effect on chlorophylls, whereas 0.1–5.0 mg L^{-1} induced a progressive reduction, reaching ~31% at 5.0 mg L^{-1}.

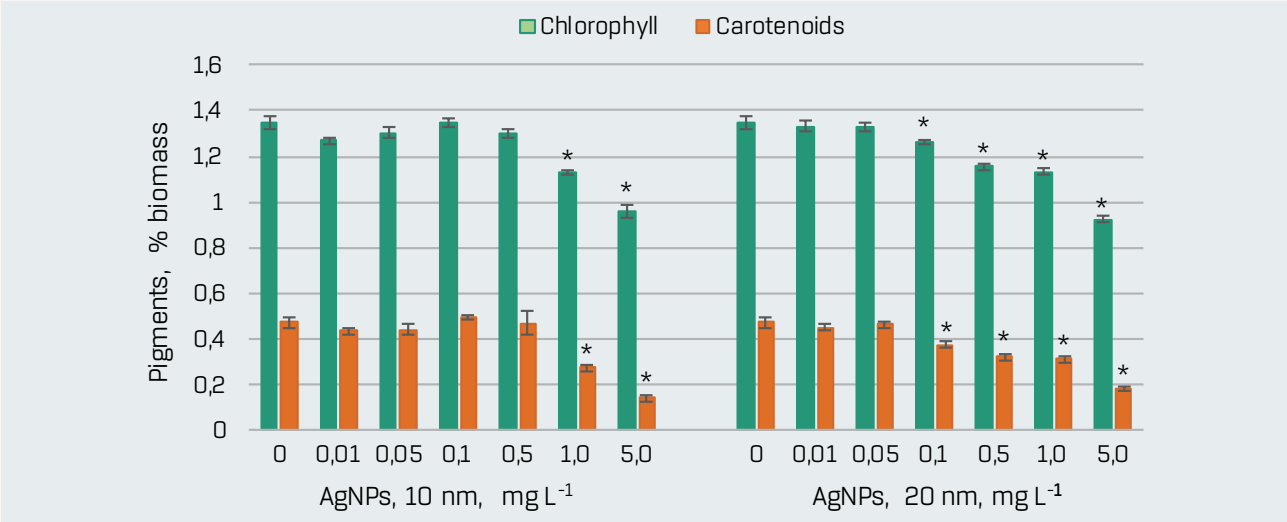

Figure 3. Total chlorophyll and carotenoid content (% biomass) in *Haematococcus lacustris* at the end of the green phase following exposure to 10 nm and 20 nm AgNPs (mg L^{-1}). 0 = control; mean ± SD (n = 3); * $p < 0.05$.

Total carotenoids followed a similar pattern. For 10 nm AgNPs, concentrations up to 0.5 mg L^{-1} did not substantially modify carotenoid levels, but 1.0 mg L^{-1} and 5.0 mg L^{-1} caused strong decreases of ~42% and ~70%, respectively. With 20 nm AgNPs, slight changes were observed at 0.01–0.05 mg L^{-1}, while 0.1–5.0 mg L^{-1} produced pronounced reductions (about 20–61%). These trends indicate that, unlike proteins and carbohydrates, photosynthetic pigments are relatively stable under low AgNP doses but highly susceptible to inhibition at ≥1.0 mg L^{-1}.

Lipid content and malondialdehyde (MDA) levels, used as indicators of carbon allocation and oxidative stress, are shown in Figure 4. In the presence of 10 nm AgNPs, lipid content increased moderately (~12%) at 0.05–0.1 mg L^{-1} and more strongly (~31–42%) at 0.5–5.0 mg L^{-1}. For 20 nm AgNPs, significant lipid stimulation (~24–65%) was observed mainly at 0.5–5.0 mg L^{-1}, whereas lower concentrations had little effect.

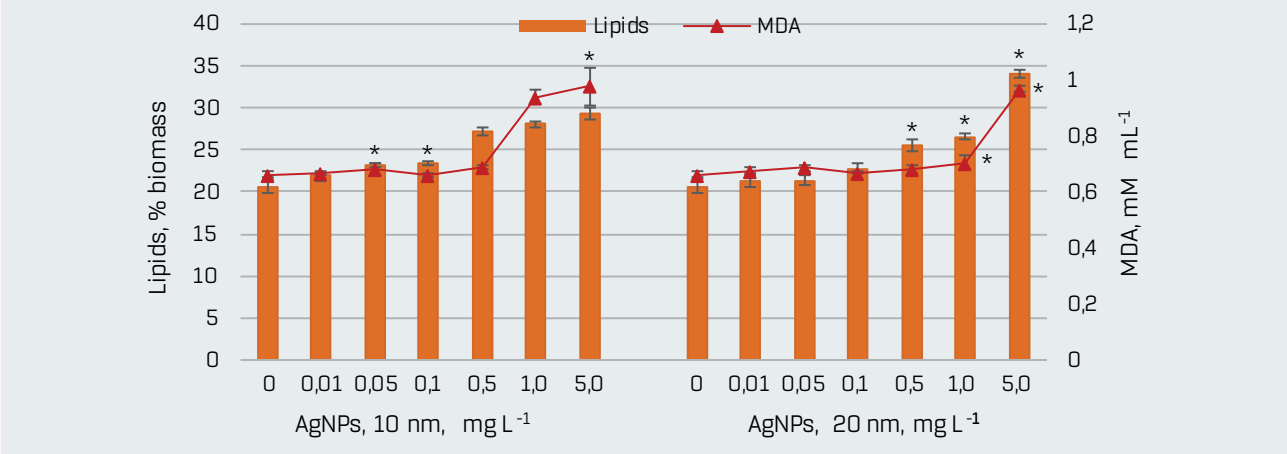

Figure 4. Lipid content (% biomass) and MDA levels (mM mL^{-1}) in *Haematococcus lacustris* at the end of the green stage following exposure to 10 nm and 20 nm AgNPs (mg L^{-1}). 0 = control; mean ± SD (n = 3); * $p < 0.05$ vs. control.

MDA levels remained close to control values at 0.01–0.5 mg L^{-1} for both nanoparticle sizes, indicating that these doses did not induce marked lipid peroxidation. However, at 1.0–5.0 mg L^{-1}, MDA increased substantially: for 10 nm AgNPs by ~42–47%, and for 20 nm AgNPs by ~6–46%. Thus, high AgNP concentrations that suppress pigments and growth are also associated with oxidative damage, whereas low–moderate doses stimulate biomass and metabolite accumulation without clear signs of stress.

Effects of AgNPs on Biomass, Astaxanthin, and Lipids in the Red Aplanospore Stage

At the red cyst (aplanospore) stage, the impact of AgNPs differed from that observed in the green phase, reflecting the shift towards stress-induced carotenoid and lipid accumulation (fig. 5, 6).

Biomass accumulation was consistently inhibited by AgNP exposure at the end of the cultivation cycle (fig. 5). Even the lowest concentrations (0.01–0.1 mg L^{-1}) caused moderate declines of ~5–7% for 10 nm AgNPs and ~4–8% for 20 nm AgNPs. At higher doses (0.5–5.0 mg L^{-1}), the reduction in aplanospore biomass became more pronounced, reaching ~10–35% for 10 nm particles and ~14–40% for 20 nm particles. These results suggest that although AgNPs can transiently stimulate biomass in the green stage, their prolonged presence ultimately limits final biomass at the red stage.

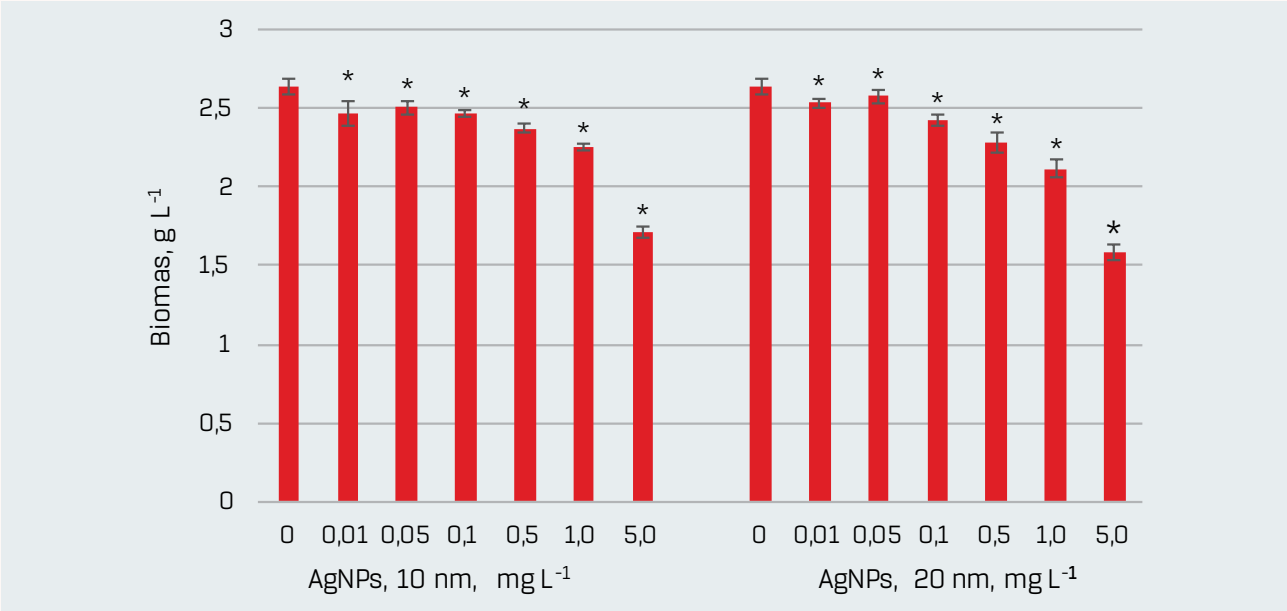

Figure 5. Biomass (g/L) of Haematococcus lacustris at the red cyst (aplanospore) stage following exposure to 10 nm and 20 nm AgNPs (mg L^{-1}). 0 = control; mean ± SD (n = 3); * $p < 0.05$ vs. control.

Astaxanthin accumulation in aplanospores exhibited a clear biphasic, concentration-dependent response (fig. 6). In cultures treated with 10 nm AgNPs, low concentrations (0.01–0.5 mg L^{-1}) stimulated astaxanthin biosynthesis, with increases of up to ~30% relative to the con-

trol, the highest value being observed at 0.1 mg L^{-1}. This indicates that mild nanoparticle-induced stress can act as a trigger for astaxanthin overproduction. Conversely, higher concentrations (1.0 and 5.0 mg L^{-1}) inhibited carotenoid accumulation, reducing astaxanthin content by ~5% and ~26%, respectively.

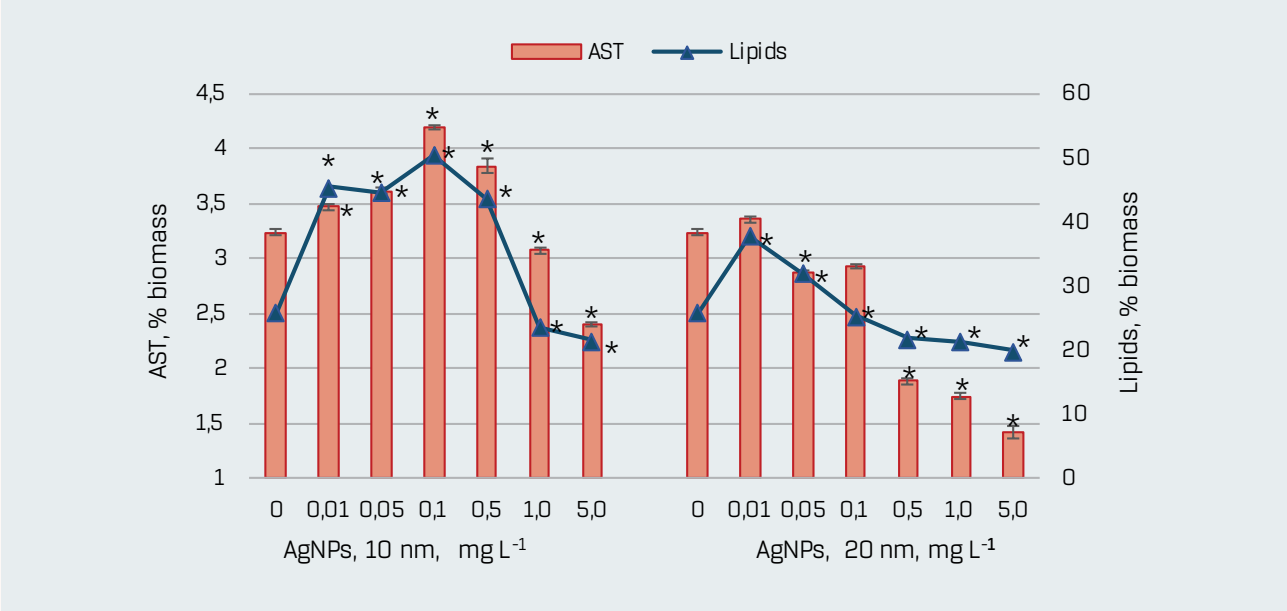

Figure 6. Astaxanthin (AST) and lipid content (% biomass) in *Haematococcus lacustris* at the aplanospore stage after exposure to 10 nm and 20 nm AgNPs (mg L^{-1}). 0 = control; mean ± SD (n = 3); * $p < 0.05$ vs. control.

For 20 nm AgNPs, the response pattern was different. Even at relatively low concentrations (0.05–0.1 mg L^{-1}), astaxanthin content already tended to decrease (by ~9–12%), and all concentrations from 0.5 to 5.0 mg L^{-1} strongly suppressed astaxanthin formation, with reductions of ~42–56%. These findings indicate that, at the aplanospore stage, 10 nm AgNPs at low–moderate doses can be exploited to enhance astaxanthin production, while 20 nm particles are largely inhibitory across the tested range.

The lipid content of aplanospores was also strongly affected by AgNPs (Figure 6). In the presence of 10 nm nanoparticles, concentrations between 0.01 and 0.5 mg L-1 markedly increased lipids, with rises of ~69–96% compared to the control, suggesting an intensified accumulation of energy-rich storage compounds in response to mild nanoparticle stress. At higher concentrations (1.0–5.0 mg L^{-1}), lipid levels declined by ~9–23%, paralleling the inhibition of astaxanthin.

For 20 nm AgNPs, lipid stimulation was restricted to the lowest concentrations (0.01–0.05 mg L^{-1}), where increases of ~24–47% were observed. At 0.5–5.0 mg L^{-1}, lipid content decreased significantly, with reductions comparable to those seen for astaxanthin (about 9–23%).

DISCUSSIONS

The present study analyzed the effects of silver nanoparticles on *Haematococcus lacustris* at two key physiological stages – green vegetative cells and red aplanospores – to reveal stage-specific metabolic responses and their relevance for astaxanthin and lipid production. Administering 10 nm and 20 nm AgNPs at the onset of the green stage enabled the evaluation of nanoparticle action during intensive biosynthesis as well as during the subsequent stress-driven transition to the red stage.

A biphasic effect on biomass formation was observed. During the green stage, low and moderate AgNP concentrations (≤1 mg L^{-1}) stimulated biomass accumulation, whereas 5 mg L^{-1} inhibited growth. Comparable stimulatory effects of low AgNP doses have been reported for *Porphyridium purpureum* and *Chlamydomonas reinhardtii* (25, 26). However, inhibition of biomass formation is the predominant outcome described in the literature, especially at ≥1 mg L-1 AgNPs, as demonstrated for *Nannochloropsis oculata, Dunaliella salina*, and several filamentous green algae (27–29). The final biomass collected at the aplanospore stage was reduced at all AgNP doses, indicating that prolonged exposure, even at low levels, ultimately constrains culture productivity. This is consistent with reports highlighting the overall high toxicity of silver nanoparticles to microalgae (30).

In the green stage, *H. lacustris* showed enhanced protein and carbohydrate content across nearly all treatments, pointing to intensified primary metabolism. Similar increases – interpreted as adaptive responses to moderate oxidative stress – were reported for *Oedogonium*, *Ulothrix, Cladophora,* and *Spirogyra* exposed to low AgNP concentrations (33). In contrast to these species, where stress-induced accumulation occurred alongside biomass inhibition, *H. lacustris* in our study exhibited metabolite increases associated with biomass stimulation, suggesting that the stress level induced by low–moderate AgNPs concentrations remained compensable during the vegetative stage.

Chlorophyll and carotenoids were more sensitive indicators of AgNP toxicity. Although pigment levels remained close to control values at ≤0.5 mg L^{-1}, clear declines occurred at 1–5 mg L^{-1} for both nanoparticle sizes, consistent with the well-documented suppression of photosynthetic pigments under AgNP exposure (34, 35). The carotenoid-to-chlorophyll ratio (Car/Chl), a marker of photosynthetic functionality, remained within the characteristic range for the green stage at 0.01–0.5 mg L^{-1} AgNPs, confirming maintenance of primary metabolism under low stress. In contrast, higher concentrations that reduced chlorophyll also altered the Car/Chl ratio, indicating impaired pigment homeostasis.

Lipid content exhibited concentration-dependent stimulation in the green stage, reflecting adaptive remodeling of membrane systems under stress, a phenomenon widely described for microalgae exposed to adverse conditions (8, 37, 38). The increase in lipids observed at both nanoparticle sizes suggests activation of compensatory responses, while elevated MDA levels at ≥1 mg L^{-1} indicate that excessive nanoparticle doses trigger oxidative damage. The correlation between lipids and MDA supports this interpretation.

At the aplanospore stage, the metabolic pattern changed. Low concentrations of 10 nm AgNPs stimulated astaxanthin accumulation, while higher doses inhibited it. Published data similarly describe both suppressive and stimulatory effects of AgNPs on astaxanthin, depending on dose, exposure duration, and physiological state (21, 31). In our study, 20 nm AgNPs caused inhibition at nearly all concentrations, highlighting that nanoparticle size is an important determinant of stress sensitivity.

A strong positive correlation between total carotenoids (green stage) and astaxanthin (red stage) indicates that precursor availability influences final pigment accumulation. At the same time, the negative correlations between lipid content in green and red stages suggest dynamic redistribution of metabolic resources during stress adaptation. Lipids, which function as storage matrices for astaxanthin, showed a strong positive association with astaxanthin levels in the red stage, supporting the interdependence of these biosynthetic pathways.

Overall, the findings show that *H. lacustris* exhibited a clear hormetic response to silver nanoparticles. Low concentrations of 10 nm AgNPs enhanced biomass formation and stimulated the accumulation of primary metabolites, lipids, and astaxanthin, whereas higher doses surpassed the cellular tolerance threshold, resulting in pigment degradation, oxidative damage, and reduced astaxanthin synthesis. The ability of *H. lacustris* to withstand moderate stress and redirect its metabolism toward protective and storage compounds, such as carotenoids and lipids, highlights its adaptive plasticity and suggests opportunities for controlled metabolic enhancement, provided nanoparticle exposure remains within non-inhibitory ranges.

These stage-dependent responses underscore the importance of nanoparticle dose, size, and timing of application in determining whether their effects are stimulatory or toxic.

CONCLUSIONS

1. This study has proved that silver nanoparticles induced distinct, stage-specific responses in *Haematococcus lacustris*, with direct implications for biomass accumulation, astaxanthin synthesis, and cellular metabolite profiles.
2. Low to moderate concentrations of 10 nm AgNPs stimulated biomass production during the green stage and enhanced lipid and astaxanthin accumulation during the red aplanospore stage, suggesting that controlled nanoparticle-induced stress can be exploited to boost valuable metabolites. In contrast, higher concentrations of 10 nm AgNPs and all tested doses of 20 nm AgNPs markedly suppressed biomass and astaxanthin production, indicating increased toxicity associated with larger particle size and elevated exposure levels.

3. These findings confirmed a hormetic response, in which metabolic stimulation was restricted to a narrow exposure window, while excessive nanoparticle-induced oxidative stress led to inhibitory effects.
4. Overall, this knowledge has provided a scientific basis for developing controlled, nanoparticle-assisted strategies to enhance microalgal bioproduct yields while minimizing adverse toxic effects.

ETHICAL APPROVAL

Was not required for this study, as the research did not involve human participants, animals, or interventions subject to ethical committee review.

CONFLICT OF INTEREST

The authors declare no conflicts of interest. The funders had no role in the design of the study; in the collection, analyses, or interpretation of data; in the writing of the manuscript; or in the decision to publish the results.

AUTHOR CONTRIBUTIONS

Conceptualization, L.C. and L.R.; methodology, L.R., T.C. and V.M.; investigation, V.M., T.C. and E. P.; data curation, L.R.; writing – original draft preparation, L.C. and T.C; writing – review and editing L.C.; project administration, L.C. All authors have read and agreed to the published version of the manuscript.

FUNDING

This research was funded by National Agency for Research and Development, Republic of Moldova, Project 24.80012.7007.08 SE" Oxidative stress as a tool in production of microalgae derived antioxidant astaxanthin".

REFERENCES

1. Bayda S, Adeel M, Tuccinardi T, Cordani M, Rizzolio F. The History of Nanoscience and Nanotechnology: From Chemical–Physical Applications to Nanomedicine. *Molecules*. 2019;25(1):112. https://doi.org/10.3390/molecules25010112
2. Malik S, Muhammad K, Waheed Y. Nanotechnology: A Revolution in Modern Industry. *Molecules*. 2023;28(2):661. https://doi.org/10.3390/molecules28020661
3. Kumah EA, Fopa RD, Harati S, Boadu P, Zohoori FV, Pak T. Human and environmental impacts of nanoparticles: a scoping review of the current literature. *BMC Public Health*. 2023;23(1):1059. https://doi.org/10.1186/s12889-023-15958-4
4. Iavicoli I, Leso V, Fontana L, Calabrese E. Nanoparticle Exposure and Hormetic Dose–Responses: An Update. *IJMS*. 2018;19(3):805. https://doi.org/10.3390/ijms19030805
5. Reetu, Clifford M, Prakash R, Rai MP. Latest advances and status analysis of nanomaterials for microalgae photosystem, lipids and biodiesel: A state of art. *Journal of Environmental Chemical Engineering*. 2023;11(1):109111. https://doi.org/10.1016/j.jece.2022.109111
6. Yuan X, Gao X, Liu C, et al. Application of Nanomaterials in the Production of Biomolecules in Microalgae: A Review. *Marine Drugs*. 2023;21(11):594. https://doi.org/10.3390/md21110594
7. Liu Y, Wang S, Wang Z, Ye N, Fang H, Wang D. TiO2, SiO2 and ZrO2 Nanoparticles Synergistically Provoke Cellular Oxidative Damage in Freshwater Microalgae. *Nanomaterials*. 2018;8(2):95. https://doi.org/10.3390/nano8020095
8. Vargas-Estrada L, Torres-Arellano S, Longoria A, Arias DM, Okoye PU, Sebastian PJ. Role of nanoparticles on microalgal cultivation: A review. *Fuel*. 2020;280:118598. https://doi.org/10.1016/j.fuel.2020.118598
9. Déniel M, Errien N, Daniel P, Caruso A, Lagarde F. Current methods to monitor microalgae-nanoparticle interaction and associated effects. *Aquatic Toxicology*. 2019;217:105311. https://doi.org/10.1016/j.aquatox.2019.105311
10. Alishah Aratboni H, Rafiei N, Mehdizadeh Allaf M, et al. Nanotechnology: An outstanding tool for increasing and better exploitation of microalgae valuable compounds. *Algal Research*. 2023;71:103019. https://doi.org/10.1016/j.algal.2023.103019
11. Huang Y, Gao M, Wang W, et al. Effects of manufactured nanomaterials on algae: Implications and applications. *Front Environ Sci Eng*. 2022;16(9):122. https://doi.org/10.1007/s11783-022-1554-3
12. Mularczyk M, Michalak I, Marycz K. Astaxanthin and other Nutrients from Haematococcus pluvialis – Multifunctional Applications. *Marine Drugs*. 2020;18(9):459. https://doi.org/10.3390/md18090459
13. Oslan SNH, Tan JS, Oslan SN, et al. Haematococcus pluvialis as a Potential Source of Astaxanthin with Diverse Applications in Industrial Sectors: Current Research and Future Directions. *Molecules*. 2021;26(21):6470. https://doi.org/10.3390/molecules26216470
14. Abdelazim K, Ghit A, Assal D, et al. Production and therapeutic use of astaxanthin in the nanotechnology era. *Pharmacol Rep*. 2023;75(4):771-790. https://doi.org/10.1007/s43440-023-00488-y
15. Dang Y, Li Z, Yu F. Recent Advances in Astaxanthin as an Antioxidant in Food Applications. *Antioxidants*. 2024;13(7):879. https://doi.org/10.3390/antiox13070879
16. Sun L, Li Y, Yang A, Xie M, Xiong R, Huang C. Astaxanthin: A comprehensive review of synthesis, biological activities and applications. *Food Chemistry*. 2025;488:144847. https://doi.org/10.1016/j.foodchem.2025.144847
17. Lutzu GA, Concas A, Damergi E, Chen L, Zhang W, Liu T. Production of Carotenoids and Astaxanthin from Haematococcus pluvialis Cultivated Under Mixotrophy Using Brewery Wastewater: Effect of Light Intensity and Cultivation Time. *Applied Sciences*. 2024;14(21):9704. https://doi.org/10.3390/app14219704
18. Samhat K, Kazbar A, Takache H, et al. Optimization of continuous astaxanthin production by Haematococcus pluvialis in nitrogen-limited photobioreactor. *Algal Research*. 2024;80:103529. https://doi.org/10.1016/j.algal.2024.103529
19. Zarei Z, Zamani H. Biorefinery approach to stimulate astaxanthin and biofuel generation in microalga Haematococcus pluvialis under different light irradiance. *Clean Techn Environ Policy*. 2024;26(10):3333-3347. https://doi.org/10.1007/s10098-024-02803-4
20. Do TT, Ong BN, Le TL, et al. Growth of Haematococcus pluvialis on a Small-Scale Angled Porous Substrate Photobioreactor for Green Stage Biomass. *Applied Sciences*. 2021;11(4):1788. https://doi.org/10.3390/app11041788
21. Venckus P, Endriukaitytė I, Čekuolytė K, Gudiukaitė R, Pakalniškis A, Lastauskienė E. Effect of Biosynthesized Silver Nanoparticles on the Growth of the Green Microalga Haematococcus pluvialis and Astaxanthin Synthesis. *Nanomaterials*. 2023;13(10):1618. https://doi.org/10.3390/nano13101618
22. Lowry OliverH, Rosebrough NiraJ, Farr AL, Randall RoseJ. Protein measurement with the folin phenol reagent. *Journal of Biological Chemistry*. 1951;193(1):265-275. https://doi.org/10.1016/S0021-9258(19)52451-6
23. Lichtenthaler HK, Wellburn AR. Determinations of total carotenoids and chlorophylls *a* and *b* of leaf extracts in different solvents. *Biochemical Society Transactions*. 1983;11(5):591-592. https://doi.org/10.1042/bst0110591
24. Park J, Jeong HJ, Yoon EY, Moon SJ. Easy and rapid quantification of lipid contents of marine dinoflagellates using the sulpho-phospho-vanillin method. *ALGAE*. 2016;31(4):391-401. https://doi.org/10.4490/algae.2016.31.12.7

25. Rudi L, Cepoi L, Chiriac T, Djur S, Valuta A, Miscu V. Effects of Silver Nanoparticles on the Red Microalga Porphyridium purpureum CNMN-AR-02, Cultivated on Two Nutrient Media. *Marine Drugs*. 2024;22(5):208. https://doi.org/10.3390/md22050208

26. Sendra M, Yeste MP, Gatica JM, Moreno-Garrido I, Blasco J. Direct and indirect effects of silver nanoparticles on freshwater and marine microalgae (Chlamydomonas reinhardtii and Phaeodactylum tricornutum). *Chemosphere*. 2017;179:279-289. https://doi.org/10.1016/j.chemosphere.2017.03.123

27. Fazelian N, Movafeghi A, Yousefzadi M, Rahimzadeh M, Zarei M. Impact of silver nanoparticles on the growth, fatty acid profile, and antioxidative response of Nannochloropsis oculata. *Acta Physiol Plant*. 2020;42(7):126. https://doi.org/10.1007/s11738-020-03101-4

28. Dash A, Singh AP, Chaudhary BR, Singh SK, Dash D. Effect of Silver Nanoparticles on Growth of Eukaryotic Green Algae. *Nano-Micro Lett*. 2012;4(3):158-165. https://doi.org/10.1007/BF03353707

29. Johari SA, Sarkheil M, Behzadi Tayemeh M, Veisi S. Influence of salinity on the toxicity of silver nanoparticles (AgNPs) and silver nitrate (AgNO3) in halophilic microalgae, Dunaliella salina. *Chemosphere*. 2018;209:156-162. https://doi.org/10.1016/j.chemosphere.2018.06.098

30. Lau ZL, Low SS, Ezeigwe ER, et al. A review on the diverse interactions between microalgae and nanomaterials: Growth variation, photosynthetic performance and toxicity. *Bioresource Technology*. 2022;351:127048. https://doi.org/10.1016/j.biortech.2022.127048

31. Cepoi L, Rudi L, Chiriac T, Plingau E, Valuta A, Miscu V. The effect of silver nanoparticles on the microalgae haematococcus pluvialis. In: Proceedings of the 16th International Conference on Nanomaterials – Research & Application (NANOCON 2024), Brno, Czech Republic, 16–18 October 2024.2025:220-225. https://doi.org/10.37904/nanocon.2024.5021

32. Shah MdMR, Liang Y, Cheng JJ, Daroch M. Astaxanthin-Producing Green Microalga Haematococcus pluvialis: From Single Cell to High Value Commercial Products. *Front Plant Sci*. 2016;7. https://doi.org/10.3389/fpls.2016.00531

33. Hasnain M, Munir N, Abideen Z, Dias DA, Aslam F, Mancinelli R. Applying Silver Nanoparticles to Enhance Metabolite Accumulation and Biodiesel Production in New Algal Resources. *Agriculture*. 2022;13(1):73. https://doi.org/10.3390/agriculture13010073

34. Pham TL. Effect of Silver Nanoparticles on Tropical Freshwater and Marine Microalgae. *Journal of Chemistry*. 2019;2019:1-7. https://doi.org/10.1155/2019/9658386

35. Liu W, Majumdar S, Li W, Keller AA, Slaveykova VI. Metabolomics for early detection of stress in freshwater alga Poterioochromonas malhamensis exposed to silver nanoparticles. *Sci Rep*. 2020;10(1):20563. https://doi.org/10.1038/s41598-020-77521-0

36. Solovchenko AE, Chivkunova OB, Maslova IP. Pigment composition, optical properties, and resistance to photodamage of the microalga Haematococcus pluvialis cultivated under high light. *Russ J Plant Physiol*. 2011;58(1):9-17. https://doi.org/10.1134/S1021443710061056

37. Alishah Aratboni H, Rafiei N, Garcia-Granados R, Alemzadeh A, Morones-Ramírez JR. Biomass and lipid induction strategies in microalgae for biofuel production and other applications. *Microb Cell Fact*. 2019;18(1):178. https://doi.org/10.1186/s12934-019-1228-4

38. Wang F, Liu T, Guan W, et al. Development of a Strategy for Enhancing the Biomass Growth and Lipid Accumulation of Chlorella sp. UJ-3 Using Magnetic Fe3O4 Nanoparticles. *Nanomaterials*. 2021;11(11):2802. https://doi.org/10.3390/nano11112802

39. Mattson MP, Calabrese EJ, eds. *Hormesis: A Revolution in Biology, Toxicology and Medicine.* Humana Press; 2010. https://doi.org/10.1007/978-1-60761-495-1

Date of receipt of the manuscript: 10.12.2025

Date of acceptance for publication: 18.12.2025

Liliana Cepoi, WoS Researcher ID: J-9640-2019, SCOPUS ID 55246094000;

Ludmila Rudi, WoS Researcher ID: AAY-3219-2020, SCOPUS ID 55681134100;

Tatiana Chiriac, WoS Researcher ID: AIB-8864-2022, SCOPUS ID 38861074900;

Vera Miscu, SCOPUS ID 55681134100.